Hierarchical Pattern Formation in Thin Film Diblock Copolymers above the Order−Disorder Transition Temperature

R. Limary and P. F. Green*

Department of Chemical Engineering and Texas Materials Institute, The University of Texas at Austin, Austin, Texas 78712

Received April 21, 1999; Revised Manuscript Received September 3, 1999

ABSTRACT: Thin symmetric poly(styrene-*b*-methyl methacrylate) (PS-*b*-PMMA) diblock copolymer films at temperatures higher than the bulk order−disorder transition temperature T_{ODT} are shown to dewet silicon substrates, forming topographical features that depend on the initial film thickness h. Films of thickness $h < 3.5$ nm dewet the substrate, forming bicontinuous spinodal-like patterns. When 3.5 nm $< h < h_L = 7$ nm, discrete holes are observed randomly throughout the film. For films of thickness in the range $h_L < h < h_H = 35$ nm, the copolymer exhibited autophobic behavior, whereby the top layer of thickness $(h - h_L)$ dewets a dense "brush" of ordered copolymer of height h_L anchored to the silicon substrate. The morphologies, which include a bicontinuous spinodal pattern for films of thickness in the range $h_L < h < 19$ nm, and discrete holes, for films of thickness in the range 19 nm $< h < h_H$, eventually evolve into droplets. Films of $h > 35$ nm remained stable, with smooth surfaces. The time-dependent evolution of the "spinodal" structures that evolve in the autophobic regime is discussed. In addition, the existence of surface-induced ordering of the copolymer at temperatures above the bulk T_{ODT} is also discussed.

Introduction

Two equilibrium situations are typically encountered when a simple liquid or a polymeric liquid droplet is on a solid substrate. In one case, partial wetting is observed where a finite equilibrium contact angle θ_e exists between the edge of the droplet and the substrate at the contact line. The other situation is complete wetting, $\theta_e = 0$, where a macroscopic film of finite thickness remains on the substrate. The contact angle is determined by Young's equation $\gamma_{sv} = \gamma_{sl} + \gamma_{lv} \cos \theta_e$, where γ_{sv} is the interfacial energy between the surface and the vapor phase, γ_{lv} is the liquid/vapor interfacial tension, and γ_{ls} is liquid/solid interfacial tension. The condition of partial or complete wetting is dictated by the spreading coefficient $S = \gamma_{sv} - (\gamma_{lv} + \gamma_{sl})$. For $S < 0$ the situation of partial wetting is observed, whereas $S > 0$ corresponds to complete wetting. Hence, the equilibrium shape of a small liquid droplet on a substrate is determined, largely, by the capillary forces.[1] If the droplet is large, then gravitational forces play an important role in determining the equilibrium height of the droplet.

For sufficiently thin films, on the order of a few nanometers, long-range intermolecular forces become significant. A thin, nonwetting, liquid film on a substrate is subject to surface undulations due to, e.g., thermally excited capillary waves.[2,3] If the film is sufficiently thin (<100 nm), the undulations can become amplified due to long-range dispersive van der Waals and other short-range molecular forces. The long-range van der Waals contribution toward the free energy of the film is

$$P(h) = -A/(12\pi h^2) \tag{1}$$

In this equation, A is the Hamaker constant. The excess intermolecular interactions or disjoining pressure $\Pi(h) = -\partial P(h)/\partial h$ tends to destabilize the film when $A > 0$. If Π increases with an increase in film thickness, any spontaneous deformation of the surface results in a pressure gradient (flow of material from thinner to thicker regions) and can result in rupturing and subsequent dewetting of the films.

The thermally induced thickness modulations created at the liquid−air interface of thin liquid films on substrates can be approximated by a sinusoidal expression $z(x,t) = h + \delta h e^{iqx}$, where the oscillatory amplitude of the surface fluctuations $\delta h = \delta h_0 e^{t/\tau}$ with wavelength $\lambda = 2\pi/q$.[4] Here x denotes the coordinate parallel to the surface, h is the initial uniform film thickness, q is the wave vector, t is the time, and τ is the relaxation time. For an unstable thin liquid film on a solid substrate, the linearized capillary wave instability model[3,4] predicts that the initial fluctuations of the film surface are amplified exponentially with a fastest growing wave vector

$$q_m = \sqrt{3/2}(a/h^2) \tag{2}$$

and a relaxation time of the instability

$$\tau_m = \pi^2 \eta \gamma h^5/|A|^2 \tag{3}$$

where a is a molecular length defined by $a^2 = |A|/6\pi\gamma$. η is the viscosity of the film and γ is the surface tension.

The morphology of destabilized films may range from characteristic bicontinuous "spinodal" patterns to discrete cylindrical holes, as determined by a combination of long- and short-range intermolecular forces.[5] Periodic surface modulations that form a bicontinuous pattern characterize "spinodal" dewetting.[5−10] These interconnected hills and valleys develop both laterally and longitudinally. The film rupturing process is driven by surface energy, and hills will grow at the expense of the valleys, conserving volume. These patterns are analogous to the spinodal images exhibited by mixtures that phase separate after being quenched deep in the two-phase region of the phase diagram.[11] Here the spinodal

10.1021/ma9906074 CCC: $18.00
Published on Web 11/05/1999

pattern is revealed by variations in composition, whereas for the spinodal dewetting the relevant order parameter is the local film thickness.

The other morphology involves the nucleation of discrete holes. These holes grow initially without rims, but later the excavated materials displaced to form the hole accumulate at the hole periphery to form rims.[3,9,12] The growth of the holes surrounded by elevated outer rims is driven by interfacial and hydrodynamic forces. The holes grow until the rims impinge, consequently forming liquid ribbons that break up into droplets due to a Rayleigh instability.

To date, experiments and theory have concentrated primarily on the dewetting of simple polymeric liquid films. Little is understood about the dewetting of stuctured fluids such as block copolymers. In this paper, we show that a diblock copolymer film above its bulk order−disorder transition temperature T_{ODT} undergoes a surface-induced ordering and subsequently dewets in an autophobic manner. Depending on thickness h of the film, the surface patterns vary from holes to bicontinuous spinodal patterns. When h is beyond a certain height, $h_H = 35$ nm, the film is stable and its surface remains smooth. The surface-induced ordering and the dewetting dynamics in the autophobic regime are discussed in detail in this paper.

Experimental Section

Thin films with thickness between 3 and 45 nm were prepared by spin-coating a toluene solution of a symmetric PS-*b*-PMMA diblock copolymer ($N = N_{PS} + N_{PMMA} = 201$; $M_w/M_n = 1.14$) from Polysciences, Inc., onto silicon substrates. The copolymer films were flat and smooth, exhibiting no topographical features, when spun from solution. Bulk symmetric diblock copolymers undergo a transition from a disordered phase to an ordered lamellar phase below the order−disorder transition temperature T_{ODT}. This event is dictated by the condition $\chi N > 10.495$,[13] where χ is the Flory−Huggins interaction parameter and N is the total degree of polymerization of the copolymer. The Flory interaction parameter χ for this copolymer is 0.0372,[14] indicating that a bulk sample of this copolymer is disordered ($\chi N = 7.4$).

The silicon substrates on which the films were cast had native SiO_x layers of approximately 2 nm on the surfaces, as determined by spectroscopic ellipsometry. The films were scored to expose the underlying substrate. This step was performed prior to annealing in order to create a reference for thickness measurements. The films were subsequently annealed at 170 °C in a vacuum oven for various times. The samples were removed periodically, quenched to room temperature, and probed with the Autoprobe CP atomic force microscopy (AFM) from Park Scientific. Ex-situ images of the surface morphologies of the films were made with the AFM operated in the contact mode. The kinetic study of the dewetting process was accomplished by examining the same region of a given sample after each heat treatment. The depth and height of the surface features relative to the substrate were determined by probing the scored edge of the film and using the exposed silicon substrate as a reference point.

Results and Discussion

This section is divided into three parts. We first discuss the patterns that are formed in films of varying thicknesses h. The second section includes discussions of surface-induced ordering in the copolymer and autophobic dewetting. In the third section, the kinetics of the structural evolution of the spinodal dewetting process in the autophobic regime is discussed.

Film Thickness-Dependent Pattern Development. A bicontinuous spinodal-like morphology is observed for films of thickness $h < 3.5$ nm, as shown in Figure 1. An accompanying line scan for a film of initial thickness $h = 3$ nm, annealed for 30 min at 170 °C, is shown in this figure. The average spacing between peak position is approximately 0.25 μm. The average peak position spacing increased less than 25% after 30 h of annealing, indicating that the kinetics are slow.

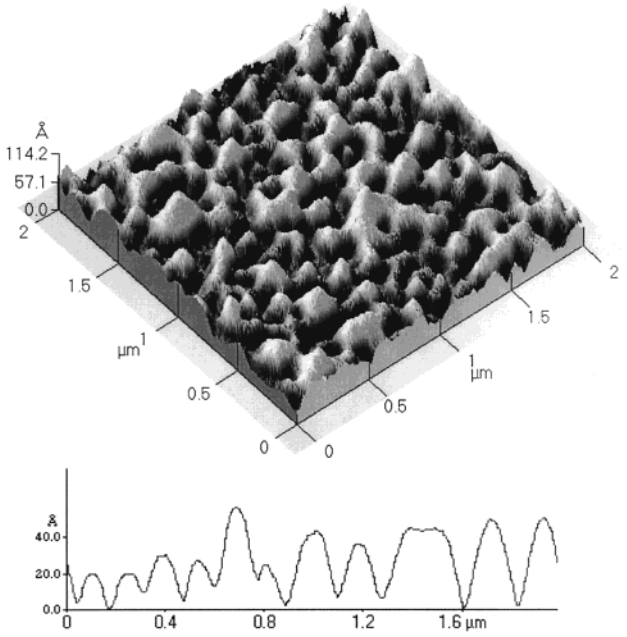

Figure 1. A 3D AFM image and an accompanying line scan of a diblock copolymer film of initial thickness $h = 3$ nm, shown after annealing for 30 min at 170 °C. A bicontinuous spinodal-like pattern is observed.

Films of 3.5 nm < h < 7 nm dewet to form a pattern of discrete cylindrical holes randomly located throughout the surface of the film, as shown in Figure 2. The image of a thin film of $h = 4$ nm was taken after the sample was annealed for 34 h at 170 °C. The characteristic rims that are generally documented for systems that dewet by a nucleation and growth mechanism[9,12] were not observed for these holes even after 34 h of annealing. The line profile in Figure 2 shows that the holes penetrate to the substrate. This was determined by scoring the edge of the film, thereby exposing the substrate. The location of the substrate was used as a reference point.

Another hierarchy of dewetting patterns was observed in this diblock copolymer when the initial film thickness was $h_L = 7$ nm < h < 19 nm. In this situation, autophobic behavior was observed. Here a copolymer layer of thickness ($h - h_L$) dewets a dense "brush" of the copolymer of height h_L. The AFM images shown in Figures 3 and 4 illustrate stages of the progression of the dewetting process. Figure 3a shows the 3D topography accompanied by a line profile of the bicontinuous spinodal-like pattern of a block copolymer film of thickness 10 nm on the "brush". The line scan indicates that the modulations occur on a "brush" of height $h_L = 7$ nm above the solid silicon substrate. The pattern eventually evolves into droplets, as shown in Figure 3b. The equilibrium contact angle that the droplets make with the copolymer brush at the line of contact was determined from AFM line profiles to be approximately 1°, with a typical droplet base diameter of 5 μm and height 40 nm for a film of initial thickness $h = 18$ nm.

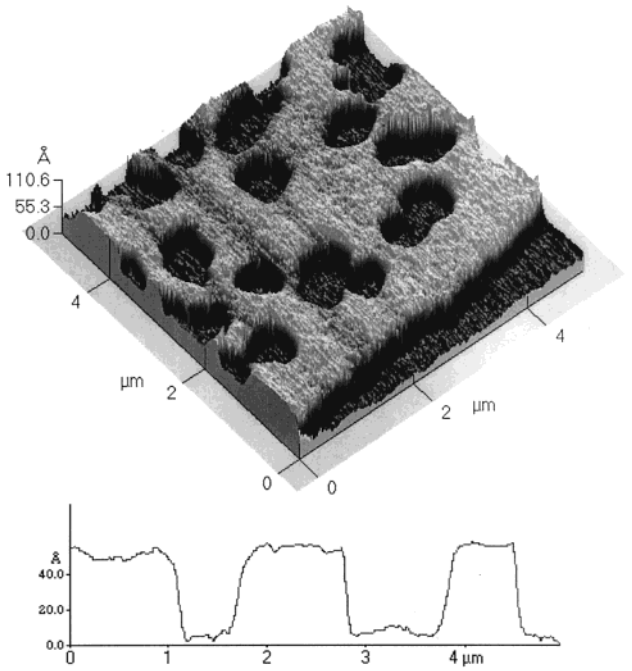

Figure 2. An AFM image and an accompanying line scan of a diblock copolymer film of initial thickness $h = 4$ nm, shown after annealing for 34 h at 170 °C. Cylindrical holes are randomly distributed throughout the sample. The line scan shows the depth of the holes and the thickness at the edge of the film, which had been scored to expose the silicon substrate prior to annealing.

Another morphology is observed when 19 nm < h < h_H = 35 nm.[12] In this case, discrete holes form which grow and eventually form droplets on a layer of height h_L = 7 nm. For h = 25 nm, the typical droplet base diameter is 7 μm and is of height 60 nm. During the early stages of development, the rim is absent from the periphery of the hole. A characteristic outer rim eventually surrounds each hole, as shown in Figure 5 of an AFM image of a film that was annealed for 10 h at 170 °C. Films of thicknesses $h > h_H$ remained stable, and no topographical features were observed beyond days of annealing at 170 °C.

The schematic in Figure 6 summarizes the hierarchy of pattern formation observed in the system. Films of initial thickness h < 3.5 nm dewet, forming a bicontinuous spinodal-like morphology. Films in the range 3.5 nm < h < h_L = 7 nm dewet, forming holes which penetrate to the substrate. When $h_L < h <$ 19 nm, the layer of thickness ($h - h_L$) becomes unstable and dewets, forming bicontinuous patterns on a "brush" of height h_L on the substrate. When 19 nm < h < 35 nm, holes appear randomly throughout the surface of the film, and when h > 35 nm, the film is stable and the surface is smooth.

Before discussing the kinetics of structural evolution of the patterns, we will first discuss the significance of the "brush" anchored on the silicon substrate.

Surface-Induced Ordering of Diblock Films. The lamellae of symmetric diblock copolymers at $T < T_{ODT}$ typically orient parallel to the plane of the substrate because one component of the A−B diblock exhibits a preferential affinity for the substrate. Because of this relative attraction, ordering of the copolymer generally proceeds from the substrate. An alternate way of considering this behavior is that the effective A/B interactions become more repulsive in the vicinity of the

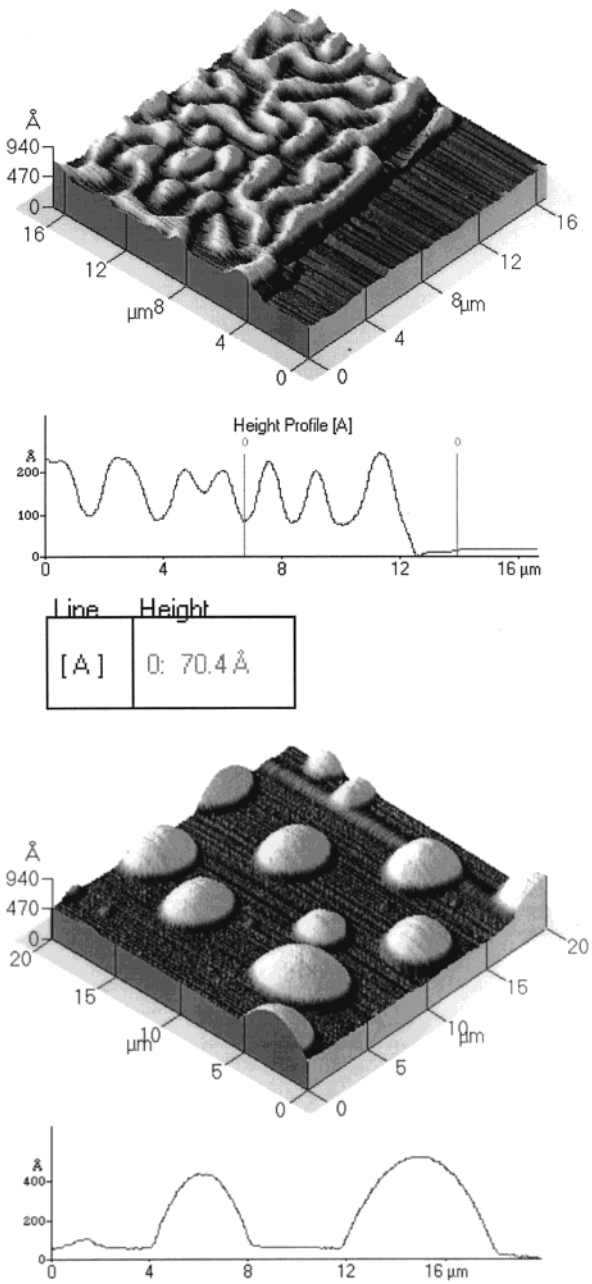

Figure 3. (a, top) A 3D AFM topographic image along with a line profile showing the undulated liquid surface after 30 min annealing at 170 °C and a region of the exposed silicon substrate (right side). This region had been scored on the sample prior to any heat treatments. The height from the valleys of the surface modulations to the reference silicon substrate is approximately 7 nm and corresponds to half of the ordered PS-*b*-PMMA interlamellar spacing. The initial local thickness of this film was 17 nm. (b, bottom) The final stage of the topography of a film with initial film thickness of 18 nm, annealed for 3680 min at 170 °C.

substrate, $\chi_{substrate} > \chi_{bulk}$.[15−17] In essence, the effective temperature at which this transition occurs is increased appreciably above the bulk value, $T_{ODT}^{substrate} > T_{ODT}^{bulk}$. Consequently, the substrate can induce ordering into the sample. By implication, the degree of segregation, particularly for weakly ordered copolymers, should be enhanced near the substrate.

In the ordered state, thin film block copolymers are known to exhibit terraces of height L, equivalent to the interlamellar spacing in the bulk. The formation of terraces,[15−17] often described as islands or holes, is

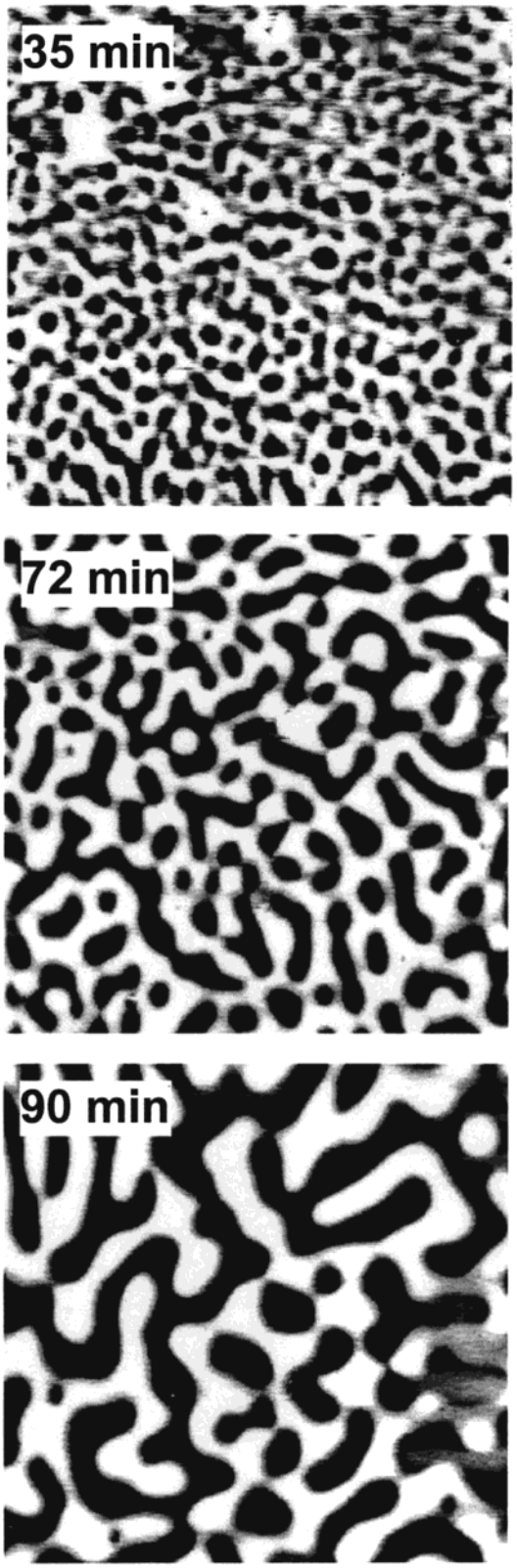

Figure 4. AFM images (20 μm × 20 μm) showing the structural evolution of spinodal dewetting patterns for a copolymer film of initial thickness $h = 18$ nm.

dictated by the commensurability between h and L. These features are created from excess materials not used to form a complete ordered layer. Studies on thin films of uniform thickness h show that if a different component is attracted to each interface, then the surface of the ordered film is smooth if $h = (n + {}^1/_2)L$,

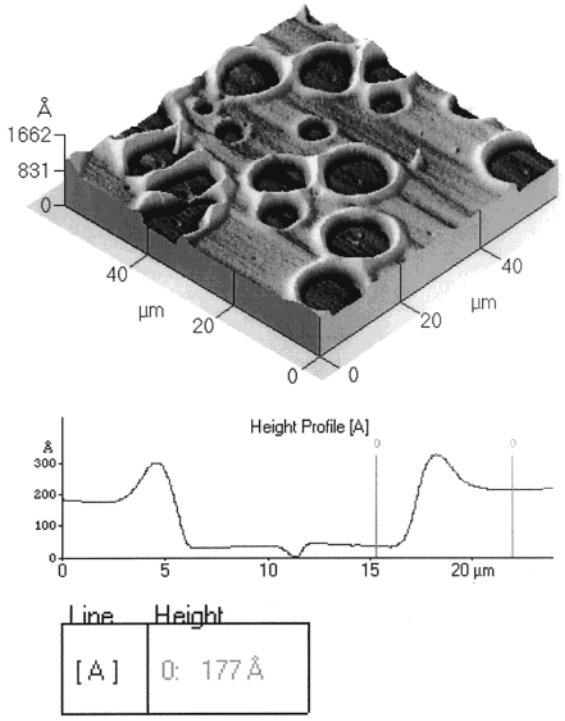

Figure 5. Topography of a film of initial thickness $h = 25$ nm, shown after 10 h of annealing at 170 °C. Note the difference in these holes from those shown in Figure 2.

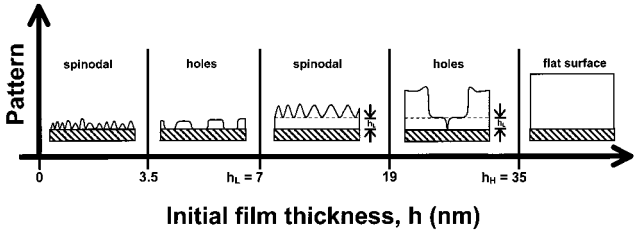

Figure 6. Surface pattern as a function of initial film thicknesses in PS-*b*-PMMA diblock copolymer. These films were annealed at 170 °C, a temperature above the isotropic to lamellar transition temperature. The topography of the films prior to annealing is flat.

where n is an integer. On the other hand, when $h = nL + \delta h$, or $h = (n + {}^1/_2)L + \delta h$, then the circular depressions form when $L/2 < \delta h < L$, whereas islands form when $0 < \delta h < L/2$. The edges of films can also vary in thicknesses from the interlamellar period L.

An estimate of the interlamellar spacing of the diblock copolymer can be made on the basis of information about a higher molecular weight ordered diblock copolymer of $N = 642$. At 170 °C, films of this PS-*b*-PMMA exhibit $L = 30$ nm,[17] and considering that $L \propto N^{2/3}$, $L/2$ is approximated to be about 7 nm for the same copolymer with $N = 201$. The thickness of the layer of polymer remaining on the substrate is approximately 7 nm (see Figure 3a). In essence, the PS-*b*-PMMA copolymer orders in the vicinity of the silicon substrate and forms a "brush" of dimensions equal to half of an interlamellar layer while the excess material remains unstructured and, within a certain thickness range, dewets this layer. Figure 7 illustrates this clearly. The region at the edge of a scored film is shown here, where a droplet exists on a layer of polymer. The light region in the inset is a droplet on the "brush". This image was taken of a sample during the late stages of dewetting. Its initial thickness was 25 nm, and it was annealed for 19.5 h at 170 °C.

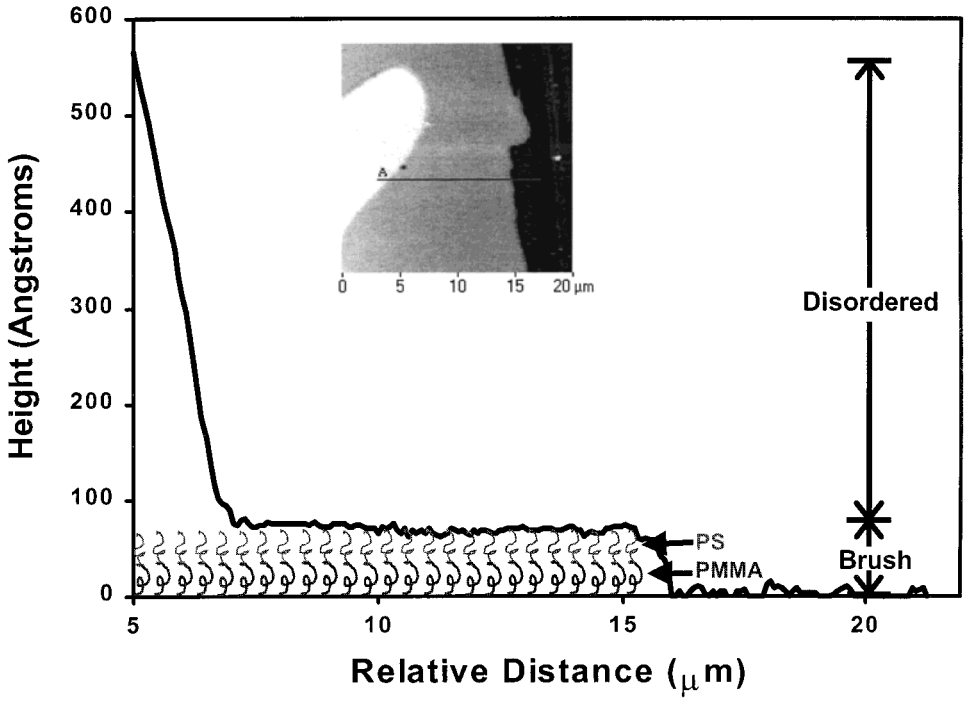

Figure 7. Schematic of a surface-induced ordered PS-*b*-PMMA ($N = 201$) diblock copolymer "brush" in contact with a disordered layer. The chains in the brush have been drawn in for illustrative purposes. Note the lower surface energy PS component is exposed to the free surface. The unstructured top layer has undergone autophobic dewetting of the "brush", as shown after 19.5 h of annealing. The line profile was taken at the edge of the film with the silicon as reference, as shown in the inset. The white region is a copolymer droplet. The right side of the image is exposed silicon.

Autophobic behavior was first documented in small molecule liquids[18] in the 1950s, and its origin in these systems is believed to be due to steric, orientation, or dipolar effects. In our case, the origins of autophobicity are primarily entropic. The layer in contact with the substrate is a dense copolymer "brush" of highly stretched chains into which the adjacent layer cannot interpenetrate. This is the well-known dry brush condition. In this situation, a nonzero interfacial tension ΔF arises at the brush/melt interface, and a partial wetting condition is created, where the spreading parameter $S = -\Delta F$.[19] We measured θ_e, the equilibrium contact angle, to be 1°, indicating that ΔF is small, as expected.

Evolution of the Spinodal Pattern in the Autophobic Regime. The evolution of the dewetting process for a film of thickness $h_L = 7$ nm $< h <$ 19 nm can be described quantitatively by a time-dependent plot of the evolution of the fastest growing q wave vector (Figure 8a). The wave vector values were determined from radial averages of 2D fast Fourier transforms (FFT) of the AFM images. The plot in Figure 8a reveals two distinct regimes of the decay of the q vector for a film of initial thickness $h = 18$ nm. In the first regime, $t < t_b = 72$ min, where t_b is the time at which the film breaks up, q undergoes a power law decay consistent with $t^{-1/3}$. Xie et al.[6] observed much slower growth for polystyrene films on silicon. However, the linearized theory of spinodal dewetting implies that q_m should be constant prior to film breakup, $2\delta h > h$.[3]

The model of spinodal decomposition in binary fluid mixtures predicts an exponent of $-1/3$ for the early diffusive growth stage.[20] Vrij[2] made an analogy between spinodal dewetting and spinodal decomposition of mixtures, where the gradients in film thickness are analogous to composition gradients in the phase-separated mixtures. However, there is a difference in the driving forces of the two phenomena. Interfacial tension between the unlike phases "drives" spinodal decomposition in mixtures,[11] whereas surface tension is responsible for the rupturing and subsequent dewetting of thin liquid films. In the absence of theory, but in analogy with spinodal decomposition, we have drawn a line indicating a $t^{-1/3}$ power law dependence. Simulations by Milchev

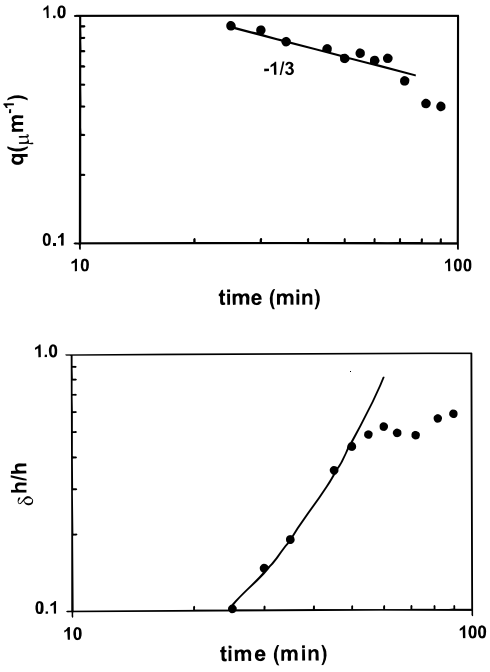

Figure 8. (a, top) Characteristic wave vector q data as a function of time. A line of $t^{-1/3}$ is drawn through the data in the first regime up to the film breakup time $t_b = 72$ min. (b, bottom) A plot illustrating the time dependence of the growth of the average amplitude of the surface undulations δh. At early times, $t < 50$ min, the amplitude grows exponentially with time.

and Binder[10] suggest a number of similarities between spinodal dewetting and spinodal decomposition. They indicate, however, that the dewetting growth exponents might be different because of the presence of the surface. In fact, their simulations suggest that at long times the dewetting kinetics should scale as $t^{-0.39}$. It should be emphasized that an accurate determination of an exponent is not possible because q does not vary over decades in this dewetting problem. While the linearized theory predicts that in this early regime q should be constant, the observation of the very early stage remains an experimental challenge since the magnitude of these undulations is comparable to that of noise.

At a transitional stage of the process, the bicontinuous pattern begins to break up, exposing the underlying surface at time $t_b \approx 72$ min. The q vector subsequently becomes more strongly time dependent. During the late stages of spinodal decomposition, hydrodynamic effects become important, and the rate of the growth of the pattern increases, exhibiting a stronger power law time dependence on t.[11] The data on PS-*b*-PMMA show a similar trend (Figure 8a).

A plot of the amplitude of the thickness modulation δh as a function of time can yield further insight into the dynamics of the dewetting process of the diblock copolymer (Figure 8b). The values for the amplitude of the undulations were obtained by averaging over line profiles of AFM topographic micrographs. The average δh increases exponentially during early dewetting, consistent with the amplitude growth observed in polystyrene.[6] A fit to the data up to $t_{dev} = 50$ min using the predictions of the dewetting model provides the average initial height amplitude $\delta h_0 \approx 0.7$ nm and relaxation time $\tau_m = 20$ min. A deviation from this exponential growth occurs for times beyond t_{dev} of annealing, where the rate decreases.

Conclusion

We examined the effect of the substrate on the topographical structures that develop at the free surface of a symmetric A−B diblock copolymer in which the B component has a strong preferential affinity for the substrate while the A component is nonwetting. These initially smooth copolymer films were annealed at temperatures above the bulk order−disorder transition temperature, T_{ODT} ($\chi N < 10.5$). The schematic in Figure 6 summarizes the hierarchy of pattern formation observed in the system. Films of initial thickness $h < 3.5$ nm dewet, forming a bicontinuous spinodal-like morphology. Films in the range 3.5 nm $< h < h_L = 7$ nm dewet, forming holes which penetrate to the substrate. When $h_L < h < 19$ nm, the layer of thickness ($h - h_L$) became unstable and dewet, forming bicontinuous patterns on a "brush" of height $h_L = L/2$ on the substrate. For 19 nm $< h <$ 35 nm, nucleation and growth of holes was the dominant mechanism, whereas films of $h >$ 35 nm were stable.

The kinetics of structural evolution of films of $h > 7$ nm (autophobic regime) was about an order of magnitude faster than films of $h < 7$ nm. The autophobic "spinodal" dewetting process (7 nm $< h <$ 19 nm) was described by a dominant wave vector which decreased with time, $q_m \sim t^{-1/3}$, while the thickness fluctuations δh grew exponentially. At later times beyond t_b, the film breakup time, the dominant wave vector decayed at a faster rate. During this time, the height fluctuations continued to increase but at a slower rate.

Acknowledgment. This work was supported by the National Science Foundation (DMR-9705101).

References and Notes

(1) de Gennes, P. G. *Rev. Mod. Phys.* **1985**, *57*, 827.
(2) Vrij, A. *Discuss. Faraday Soc.* **1966**, *42*, 23.
(3) Brochard-Wyart, F.; et al. *Langmuir* **1993**, *9*, 3682.
(4) Brochard-Wyart, F.; Daillant, J. *Can. J. Phys.* **1990**, *68*, 1084.
(5) Sharma, A.; Khanna, R. *Phys. Rev. Lett.* **1998**, *81*, 3463.
(6) Xie, R.; Karim, A.; Douglas, J. F.; Han, C. C.; Weiss, R. A. *Phys. Rev. Lett.* **1998**, *81*, 1251.
(7) Herminghaus, S.; et al. *Science* **1999**, *282*, 916.
(8) Sferrazza, M.; et al. *Phys. Rev. Lett.* **1998**, *81*, 23.
(9) Segalman, R. A.; Green, P. F. *Macromolecules* **1999**, *32*, 801.
(10) Milchev, A.; Binder, K. *J. Chem. Phys.* **1997**, *106*, 1978.
(11) Cahn, J. W. *J. Chem. Phys.* **1965**, *42*, 93.
(12) Limary, R.; Green, P. F. *Langmuir* **1999**, *15*, 5617.
(13) See for example: Bates, F. S.; Fredrickson, G. H. *Annu. Rev. Phys. Chem.* **1990**, *41*, 525.
(14) Russell, T. P.; Hjelm, R. P.; Seeger, P. A. *Macromolecules* **1990**, *23*, 890.
(15) Coulon, G.; Russell, T. P.; Deline, V. R.; Green, P. F. *Macromolecules* **1989**, *22*, 5677.
(16) See for example: Collin, B.; Chatenay, D.; Coulon, G.; Ausserre, D.; Gallot, Y. *Macromolecules* **1992**, *25*, 1621.
(17) Orso, K. A.; Green, P. F. *Macromolecules* **1999**, *32*, 1087.
(18) Hare, E.; Zisman, W. A. *J. Phys. Chem.* **1955**, *59*, 335, 1097.
(19) Shull, K. R. *Faraday Discuss.* **1998**, *98*, 203.
(20) See for example: Siggia, E. D. *Phys. Rev. A* **1979**, *20*, 595. Chen, H.; Chakrabarti, A. *Phys. Rev. E* **1997**, *55*, 5680.

MA9906074